Adaptive Look-Ahead Distance Based on an Intelligent Fuzzy Decision for an Autonomous Vehicle

Fadel Tarhini, Reine Talj, Moustapha Doumiati

Adaptive Look-Ahead Distance Based on an Intelligent Fuzzy Decision for an Autonomous Vehicle

Fadel Tarhini
CNRS, Heudiasyc UMR 7253
Université de Technologie de Compiègne
Compiègne, France
fadel.tarhini@hds.utc.fr

Reine Talj
CNRS, Heudiasyc UMR 7253
Université de Technologie de Compiègne
Compiègne, France
reine.talj@hds.utc.fr

Moustapha Doumiati
ESEO-IREENA UR4642
Nantes Université
Angers, France
moustapha.doumiati@eseo.fr

***Abstract*—Autonomous vehicles use a set of perceptual and localization data proceeding from sensor measurements, in order to plan a certain trajectory based on decision-making, and finally to track the generated path. Trajectory following is performed by adjusting the steering angle generated by a lateral controller based on a geometric or non-geometric approach. The objective of the lateral controller is to minimize the lateral error between the vehicle and the path at a target point at a look-ahead distance from the vehicle. This paper investigates the look-ahead distance due to its high impact on performance alteration, and energy consumption. An intuitive analysis will be performed to study the effect of three varying parameters on the look-ahead distance, and the necessity to consider them. Then, a Fuzzy Logic approach will be established to adjust the look-ahead distance in accordance with three parameters: longitudinal velocity, road curvature, and original consideration of road adherence. Finally, a non-geometric model-based lateral controller will be developed based on the Super-Twisting Sliding Mode Control technique to control the steering angle via the Active Front Steering. The membership functions and the rules of the inputs and output of the Fuzzy Logic approach are implemented in a Matlab/Simulink environment and tested on a validated full non-linear vehicle model. Simulation results indicate the effectiveness of the fuzzy decision approach on the performance and energy consumption of the autonomous vehicle.**

***Index Terms*—Autonomous Vehicle, Fuzzy Logic, Look-ahead Distance, Super-Twisting Sliding Mode Control**

I. Introduction

The Grand Challenge was designed to extend beyond traditional vehicle driving and tap into the ingenuity of the wider research community. Such challenges can boost research growth and attract a wide variety of researchers in correspondence to this domain. Research on Autonomous Vehicles (AVs) has been progressively accelerating since the foundation of the first DARPA Challenge in 2004 [1].

Following the decision-making based on a defined policy, the autonomous vehicle generates a path and acts toward tracking it. Path-tracking is achieved by controlling the lateral dynamics by adjusting the vehicle steering angle. [2] developed an efficient Model Predictive Control (MPC) for lateral control considering path preview to improve the robustness and computational efficiency in high-speed lateral motion control. A design was proposed for an automatic steering controller and has been implemented on an 18.3-m articulated bus for revenue service [3], where the resultant system achieved all performance requirements, and the revenue service at Eugene, OR, USA, started in June 2013. [4] presented a novel robust MPC with a finite time horizon, for the purpose of coordinating between path tracking and direct yaw moment control, while [5] designed an MPC for path following and yaw motion control. As an approach to couple the lateral and longitudinal dynamics, [6] proposed to follow a trajectory while controlling the vehicle's longitudinal velocity.

Lateral controllers can be divided into geometric controllers such as Pure Pursuit (PP) and Stanley method, and non-geometric control-theory-based controllers, like for instance model-based controllers. The objective of the lateral controllers is to minimize the lateral displacement error between the vehicle and the reference lane. Instead of immediately attempting to minimize the error from the vehicle's center of gravity, it is minimized at a target point at a look-ahead distance in front of the vehicle. The control concepts based on look-ahead systems have been researched since the 90s. Ollero proposed a method that generates the appropriate vehicle's steering angle command by combining fuzzy logic with the geometric pure-pursuit (PP) technique [7]. Four variables served as inputs in his fuzzy system: the distance from the vehicle to the nearest point, actual velocity, curvature at the target point, and the difference between vehicle heading and the heading of the nearest point in the path. [8] proposed an improved PP with an adaptive adjustment of the look-ahead distance based on the steering angle and the deflection angle. [9] proposed a non-linear relation between the look-ahead distance and the steering angle rate and the velocity. The aim was to design a controller that minimizes the steering angle rate by determining a proper look-ahead distance. [10] designed an output measurement matrix using clothoidal constraints to consider look-ahead distance in the kinematic vehicle lateral motion model. [11] proposed an adaptive Brownian motion salp swarm algorithm to optimize the look-ahead distance for the PP method.

Other recent studies have considered particular varieties of lateral controllers based on a look-ahead distance. [12] presented an MPC-based path-following controller with steering angle envelopes, and a look-ahead distance adapted to velocity variation. In order to reduce the overall monetary cost of hybrid electric vehicles, [13] proposed a look-ahead traffic information-based real-time MPC scheme where the look-ahead horizon considers vehicle-to-vehicle and vehicle-

This work has been funded by the National Agency of Research (ANR)

to-infrastructure information extraction.
Literature indicates that the look-ahead distance has often been treated based on vehicle longitudinal velocity or road curvature. Other studies considered tuning this distance in terms of one or more of the following: heading angle, steering angle, steering angle rate, lateral displacement error, lateral error at the initial conditions, etc. The look-ahead distance based on road adherence has not been the subject of any investigation, to the best of our knowledge. In this paper, a fuzzy logic approach was applied to handle three parameters that affect the look-ahead distance. These inputs were defined as the vehicle's longitudinal velocity, road curvature, and road adherence.

The paper contributions are stated as:

- For the first time, a study is conducted on the effect of road adherence on the look-ahead distance.
- Development of a novel fuzzy logic approach considering three inputs: vehicle's longitudinal velocity, road curvature, and road adherence, with the look-ahead distance as the sole output.
- Establishment of complex membership functions to guarantee smooth transitions and assign a total of 75 rules based on several simulations and driver experience.
- Conducting several tests to demonstrate the effectiveness of the proposed method in terms of vehicle stability, path tracking, and energy consumption.

The paper is structured as follows: Section II discusses lateral control based on a look-ahead distance, elaborating a set of rules based on a study of the effect of the parameters under consideration on the look-ahead distance. Section III introduces the fuzzy logic approach to determine the look-ahead distance. Results and discussion are presented in Section IV, followed by a conclusion in Section V.

II. Lateral Control based on a Look-ahead Distance Ls

The objective of attaining vehicle autonomy is a non-trivial problem. Autonomous vehicles are driven by a complex interconnection between several modules, from perception to localization, planning, and control. The objective of the latter is to regulate the lateral dynamics in order to minimize the lateral displacement error between the vehicle and a target point at a look-ahead distance Ls on the vehicle's longitudinal axis (see Fig. 1).
Unlike geometric methods, this study considered a non-geometric model-based approach for trajectory following. Lateral control is achieved using the Active Front Steering (AFS) mechanism. The AFS actuator comprises a small electric motor that generates a controlled steering angle δ_c, which is determined based on a control technique. The Super-twisting Sliding Mode Control (STSMC) is applied, which is a second-order sliding mode control. The vehicle is localized on a map formed of recorded data points, and the lateral error e_y is computed by projecting the corresponding points on the vehicle's longitudinal axis. Therefore, the objective is to drive the lateral error at a look-ahead distance ($e_{y@Ls}$) and its rate to zero. To this end, let's define the sliding variable

$$s_y = \dot{e}_{y@Ls} + k_y e_{y@Ls}, \quad \text{with } k_y > 0 \tag{1}$$

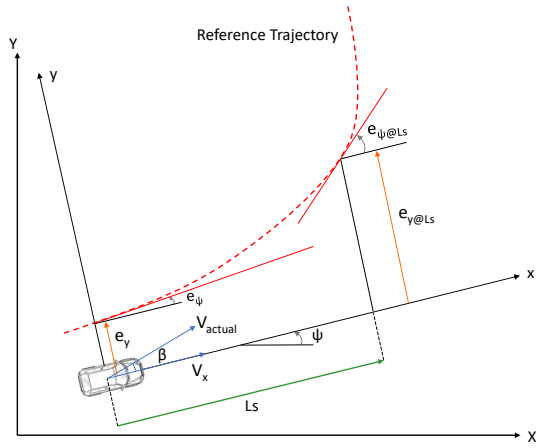

Fig. 1: Look-ahead distance

where s_y has a relative degree equal to 1 w.r.t the control input δ_c. Assume that there exist S_0, b_{min}, b_{max}, C_0, U_{max} verifying that for all x $\in \mathbb{R}^n$ and $|s(x,t)| < S_0$:

$$\begin{cases} |u(t)| \leq U_{max} \\ |\Phi(s,t)| < C_0 \\ 0 < b_{min} \leq |\xi(s,t)| \leq b_{max} \end{cases} \tag{2}$$

where $\Phi_y(s_y,t)$ and $\xi_y(s_y,t)$ are bounded functions and u is the control input. Hence,

$$\ddot{s}_y(s_y,t) = \Phi_y(s_y,t) + \xi_y(s_y,t)\dot{\delta}_c(t) \tag{3}$$

Finally, the controlled steering angle δ_c is given by

$$\delta_c = -\alpha_{\delta,1}|s_y|^{\tau_\delta} sign(s_y) - \alpha_{\delta,2}\int_0^t sign(s_y)\, d\tau, \tag{4}$$

where τ_δ is a constant in the interval]0,0.5] and $\alpha_{\delta,i}$ with i = [1,2] are positive constants satisfying the conditions

$$\begin{cases} \alpha_1 \geq \sqrt{\frac{4C_0(b_{max}\alpha_2+C_0)}{b_{min}^2(b_{min}\alpha_2-C_0)}} \\ \alpha_2 > \frac{C_0}{b_{min}} \end{cases} \tag{5}$$

The STSM control input δ_c (4) guarantees the convergence of s_y to zero in a finite time, hence $\dot{e}_{y@Ls} + k_y e_{y@Ls} \to 0$. Once reaching the sliding surface, $e_{y@Ls}$ converges exponentially to zero with a rate $k_y > 0$. The reader can refer to [14] for the convergence analysis.
Tuning the look-ahead distance Ls solely based on the velocity or road curvature is not sufficient. There is a set of complex scenarios that the autonomous vehicle can't handle. Moreover, it will be demonstrated that the look-ahead distance must be tuned with the adherence variation, in dependence on the road curvature.

A. Longitudinal Velocity V_x

Trajectory following is associated with velocity control to ensure comfortable driving. The longitudinal velocity of the vehicle is controlled to track a desired velocity profile $V_{x_{des}}$ (6) which takes into consideration the speed limit ($V_{x_{lim}}$) and comfort criteria by keeping the lateral acceleration under a maximum threshold $a_{y_{max}} = 4\ m/s^2$ as stated in [15].

$$V_{x_{des}} = \min\left(\sqrt{\frac{a_{y_{max}}}{\rho}}, V_{x_{lim}}\right) \tag{6}$$

where ρ is the road curvature. Then, longitudinal velocity control is achieved using the STSMC for V_x to track $V_{x_{des}}$. As similar to s_y, let's define

$$s_x = (V_x - V_{x_{des}}) + k_x \int (V_x - V_{x_{des}})\, dt \tag{7}$$

where $k_x > 0$. Then the control input T_m representing the total driving torque is given by

$$T_m = -\alpha_{T_m,1} |s_x|^{\tau_{T_m}} sign(s_x) - \alpha_{T_m,2} \int_0^t sign(s_x)\, d\tau, \tag{8}$$

where $\alpha_{T_m,i}$ with i = [1,2] are positive constants satisfying conditions of (5). τ_{T_m} is a constant in the interval]0,0.5].
Look-ahead systems use perceptual data extracted from vision sensors such as cameras and LiDARs to compute the lateral displacement error in front of the vehicle. Hence, there exist time delays from the sensors to the controller and the actuator. As a consequence, if Ls remains near the vehicle as the vehicle speed increases, the actuator may be unable to minimize the lateral error. Therefore, the look-ahead distance must be regulated with the velocity variation.
As Ls is incremented, the distance needed to be traveled will decrease, however, the lateral error will increase. Consequently, lower traveled distance implies lower energy consumption (see Fig. 2). On the other hand, Ls must not be excessively augmented, in order to take into consideration the possibility of near obstacles. Therefore, it is decided that as the vehicle speed raises, Ls should increase accordingly to account for time delays and to compromise between the energy consumption and the lateral error, under a certain limit to allow a reasonable time for obstacle detection.
Several studies have been conducted on tuning Ls with the velocity variation only. [3] estimated Ls manually by analyzing the closed-loop poles with respect to speed and lateral control feedback gains at different target points. Kuwata proposed a tuning strategy that adapts the look-ahead distance according to the velocity [16]. The MIT method proposed a geometric-based approach for the path-tracking problem by adjusting Ls as a function of the velocity [17]. [18] established a linear relationship between the velocity and the look-ahead distance to vary from 5 to 25.
Indeed, the desired velocity profile merely reflects its dependency on road curvature. Nevertheless, ρ can't be totally represented by V_x, which can be influenced by other traffic factors.

B. Road Curvature ρ

The road is represented by a sequence of points (way-points) and modeled by a parametric curve. The map-matching module determines the vehicle's location in relation to the points and computes the curvature of each point. The curvature estimation is adopted from [19]. The curvature of each point on the candidate's path is determined by:

$$\rho_M^i = \frac{S_M^i}{Q_M^i} \left(\rho_{P_{bf}} + \frac{(1 - q^i \rho_{P_{bf}}) \frac{\partial^2 q^i}{\partial s^2} + \rho_{P_{bf}} \frac{\partial q^i}{\partial s}^2}{{Q_M^i}^2} \right) \tag{9a}$$

$$S_M^i = sgn(1 - q^i \rho_{P_{bf}}), Q_M^i = \sqrt{\frac{\partial q^i}{\partial s}^2 + (1 - q^i \rho_{P_{bf}})^2} \tag{9b}$$

where P_{bf} represent the way-points, $\rho_{P_{bf}}$ is the curvature profile, (s, q) represent a local curvilinear coordinate system, and i is an iteration index.
A small Ls forces the system to follow the path more precisely and allows a higher amount of curvature covering. However, small Ls results in oscillation during the lane-tracking, consequently making the vehicle unstable. Whilst, a large Ls reduces overshoot as the look-ahead distance acts as a damping factor [18], however, if it exceeds a higher limit, the tracking performance will deteriorate, leading to certain phenomena such as the cutting corner (Fig. 2).

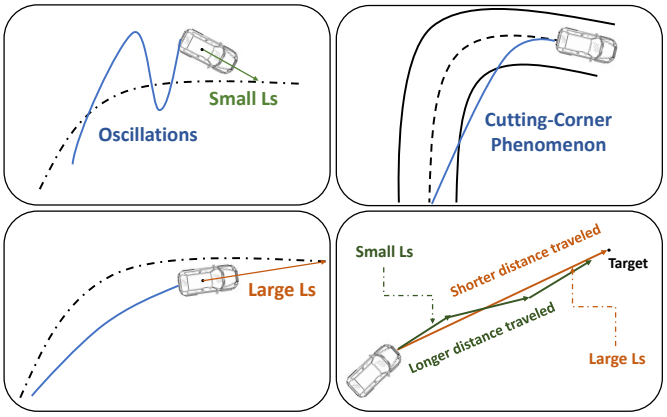

Fig. 2: Effect of Ls variation in different situations

Researchers have tended to study the effect of ρ on Ls. In order to avoid the cutting-corner problem, [20] improved the PP method, by heuristically selecting a look-ahead point by considering the relationship between a vehicle and a path, using the Dubins path algorithm. [21] extended the PP method by replacing the employed circle with a clothoid in order to decrease tracking errors. A simple feedback controller that uses vehicle lateral deviations at three look-ahead points is proposed in [22]. [23] tuned Ls by applying fuzzy logic to combine as inputs, the distance from the current location to the reference path and its changing rate.
Therefore, as road curvature increases, it is preferred to decrease the look-ahead distance to provide lower lateral errors, avoid the cutting-corner problem, and avert choosing target points outside the path. Subsequently, as road curvature decreases, reflecting a straight non-curvy road, Ls can be augmented to preclude the oscillations and lower the amount of energy consumption (see Fig. 2).

C. Road Adherence μ

Road adherence μ represents the capability of the tire to adhere to the road without slipping, or in other terms the tire-road friction. This parameter has been heavily researched due to its impact on vehicle stability, and its importance for trajectory planning. [24] presented three algorithms based on onboard sensor measurements (brake and engine torques and GPS) to estimate road adherence in real-time, and [25] proposed a framework for estimating the road friction coefficient while ensuring stability and robustness using the total aligning torque in the vehicle's front axle during steering. In this study, we considered that μ is accessible.
The lateral acceleration a_y can be related to the yaw rate $\dot{\psi}$ and the side-slip angle β by the relation (10). As the lateral stability is highly dependent on a_y, [15] proposes to maintain a_y below a threshold depending on μ.

$$a_y = V_x(\dot{\psi} + \dot{\beta}) \leq \mu g \tag{10}$$

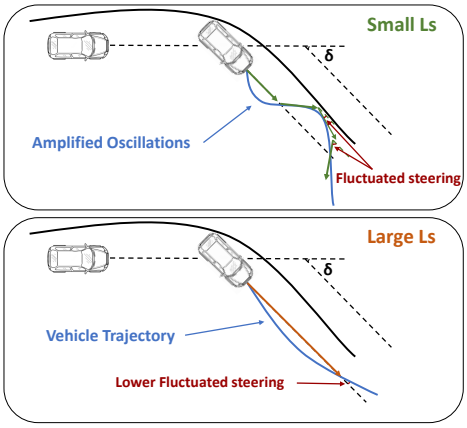

Fig. 3: Effect of Ls variation on low-adherence roads

Hence, as road adherence decreases, so does the maximal allowable lateral acceleration.

Small Ls lead to oscillations in the path-tracking of the autonomous vehicle. Due to the low friction between the tire and the road, these oscillations are amplified on low-adherence roads. Consequently, this results in a higher slip angle causing the lateral acceleration to increase. Therefore, Ls should be adapted to have higher values in the case of low-adherence roads.

Let's define two values of Ls: Ls_{min_μ}, Ls_{max_μ} representing respectively the minimum and maximum limits on low-adherence roads. On low-curvature roads, as μ decreases, it is preferred to lower the look-ahead distance in order to minimize as much as possible the lateral error to avoid unnecessary road divergence. However, Ls can be decreased to a certain limit that takes the tracking oscillations into account. Hence, on low-adherence roads, as ρ decreases to the minimum, Ls is assigned as Ls_{min_μ}, where Ls_{min_μ} increases as μ decreases. On the other hand, for high-curvature roads, the vehicle is subjected to a steering angle δ in order to track the desired path. Thus, an additional fluctuated steering reflected by the tracking oscillations to δ will result in a large lateral error and impose a high lateral acceleration leading to vehicle instability (see Fig. 3). Therefore, Ls should be increased on the high-curvature low-adherence roads. Hence, on low-adherence roads, as ρ increases to the maximum, Ls is assigned as Ls_{max_μ}, where Ls_{max_μ} increases as μ decreases.

Therefore, the look-ahead distance must be adapted to the adherence variation, which in terms depends on the road curvature. The study should be generalized by including the longitudinal velocity in order to deem the complex scenarios that the on-road vehicle may encounter. Table I summarize the rules for adapting Ls to the three parameters, where Ls_{max_V}, Ls_{max_ρ} present a compromise between energy consumption and path-tracking accuracy and respect the road

TABLE I: Look-ahead distance adaptation to V, ρ, μ

Parameter Variation	Look-ahead distance
V ↗	Ls ↗ until Ls_{max_V}
ρ ↘	Ls ↗ until Ls_{max_ρ}
μ ↘ and ρ ↘	Ls ↘ until Ls_{min_μ}; for each μ
μ ↘ and ρ ↗	Ls ↗ until Ls_{max_μ}; for each μ

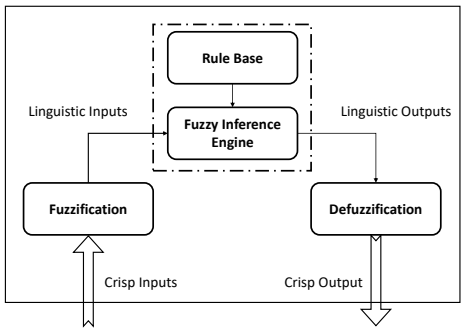

Fig. 4: Fuzzy system structure

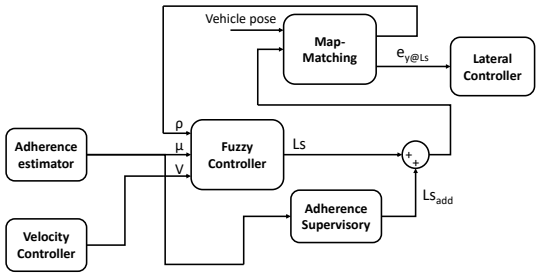

Fig. 5: Control scheme

rules, $Ls_{min_\mu} > \{Ls_{max_\rho}, Ls_{max_V}\}$, and $\{Ls_{min_\mu}, Ls_{max_\mu}\}$ increase as μ decreases.

III. Fuzzy Logic Control

The theory of the relationship between the look-ahead distance and the velocity and road curvature has not yet matured. There is no mathematical model that can relate the mentioned three variables. Besides, Ls must be adapted heuristically to road adherence. So, what is available is the performed intuitive analysis, driver experience, and data extracted from several simulations. Hence, the fuzzy logic approach is utilized in view of the fact that it does not require a complete mathematical model of the system. Furthermore, Sugeno and Nishida demonstrated the capability of fuzzy control to handle nonlinear control problems through oral instructions [26].

Fuzzy logic employs a set of rules based on expert knowledge to reach the fuzzy decision conveyed by linguistic values. The structure of the fuzzy logic system is given in Fig. 4. It consists of three stages: 1) Fuzzification where the crisp inputs are transformed into linguistic ones by computing a degree of truth for each of the input values, depending on the shape of their associated membership functions. 2) The Inference Engine is responsible for applying the defined rules to the fuzzy input in order to generate the fuzzy output. These rules are used to evaluate the linguistic values and map them to the output fuzzy set. 3) Defuzzification is the transformation of the linguistic output fuzzy values into crisp values that provide the most accurate representation of the fuzzy set.

The membership functions for the velocity V, curvature ρ, and adherence μ are shown in Fig. 6. These functions are defined as a combination of Gaussian functions to provide a smooth variation, where each Gaussian function is represented by

$$f = e^{(-\frac{(x-c)^2}{2\sigma^2})} \tag{11}$$

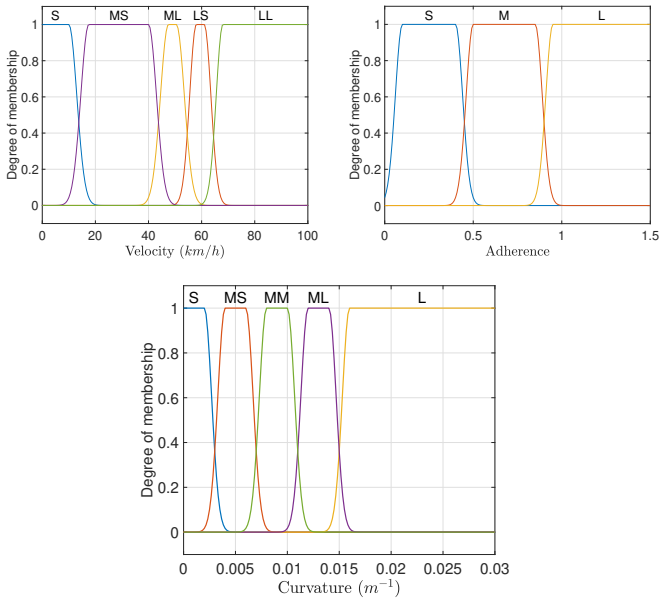

Fig. 6: Fuzzy Logic Inputs: V, μ, and ρ

where c is the mean and σ represents the standard deviation. Five fuzzy sets are defined for the velocity V: {Small (S), Medium-Small (MS), Medium-Large (ML), Large-Small (LS), Large-Large (LL)}. Three fuzzy sets for the adherence μ: {Small (S), Medium (M), Large (L)}, and five sets for the curvature ρ: {Small (S), Medium-Small (MS), Medium-Medium (MM), Medium-Large (ML), Large (L)}.
The Rule Base in the Inference Engine is established based on the driver's experience and multiple conducted simulations. Rules are defined in terms of two parameters (V, ρ) for each set of μ. Hence, there are a total of 75 rules divided into 3 tables shown in Tables II, III, IV. For each set of values for the inputs (V, ρ, μ), there exists one value for the output Ls. These values abide by the rules deducted from the analysis in section II. The fuzzy implication is solved by the Mamdani inference method (min-min-max) [27].
The membership functions of the output fuzzy variable Ls are

TABLE II: Rules for μ = L

		V				
	Ls	S	MS	ML	LS	LL
	S	ML	LS	LM	LL	HS
	MS	MM	ML	LS	LM	LL
ρ	MM	MS	MM	ML	LS	LM
	ML	SL	MS	MM	ML	LS
	L	SM	SL	MS	MM	ML

TABLE III: Rules for μ = M

		V				
	Ls	S	MS	ML	LS	LL
	S	SL	MS	MM	ML	LS
	MS	MS	MM	ML	LS	LM
ρ	MM	MM	ML	LS	LM	LL
	ML	ML	LS	LM	LL	HS
	L	LS	LM	LL	HS	HM

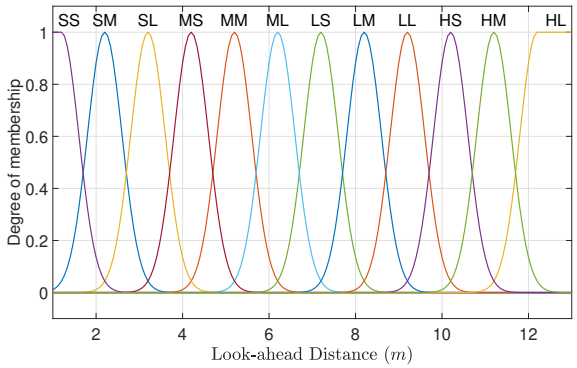

Fig. 7: Fuzzy Logic Output: Ls

TABLE IV: Rules for μ = S

		V				
	Ls	S	MS	ML	LS	LL
	S	MS	MM	ML	LS	LM
	MS	MM	ML	LS	LM	LL
ρ	MM	ML	LS	LM	LL	HS
	ML	LS	LM	LL	HS	HM
	L	LM	LL	HS	HM	HL

given in Fig. 7, in the form of Gaussian function (11). Twelve sets are defined for the look-ahead distance Ls: {ij} where i: {Small (S), Medium (M), Large (L), Huge (H)} and j: {Small (S), Medium (M), Large (L)}. Finally, the centroid method is used for the defuzzification process.
As μ decreases, the required look-ahead distance increases drastically, up until a certain limit. For $\mu = 0.5$, it has been noticed that Ls should be roughly 18 for low-curvature roads, and as it goes down, Ls should be augmented. As shown in Fig. 7, Ls ranges from 1.5 to 13. More membership functions will render the system more complex and impose more rules. Expanding the membership functions, on the other hand, will result in a greater discontinuity in Ls and reflect an instability to the vehicle. In light of this, an adherence supervisory block is inserted into the system. This block analyzes road adherence and generates an additional look-ahead distance Ls_{add} to be combined with Ls. Ls_{add} can take several values and increases as μ decreases. Further, if μ decreases below a minimum threshold μ_{min} reflecting a terrible road condition, then the effect of varying Ls dwindles. In this case, the supervisory block assigns 0 to Ls_{add} and requests an emergency braking. The complete control scheme is shown in Fig. 5.

IV. Results and Discussion

The proposed approach was implemented in Simulink/MatLab and tested on a vehicle full nonlinear model developed and validated in [28]. In order to have a better insight into the effect of Ls variation, three cost variables were introduced. The Root Mean Square (RMS) of the lateral error e_y, defined by $\sqrt{\frac{1}{T}\int_0^T e_y^2\,dt}$, the maximum lateral error, and the total energy consumed by the vehicle at the end of the test, computed by accumulating the energy at each time-step ($E_i = \frac{T\omega}{\eta}$), where T, ω, η respectively represent the torque, rotational velocity, and the efficiency of the motor.

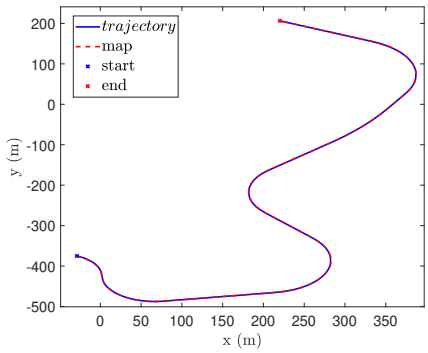

Fig. 8: Trajectory for (Sc1) and (Sc2)

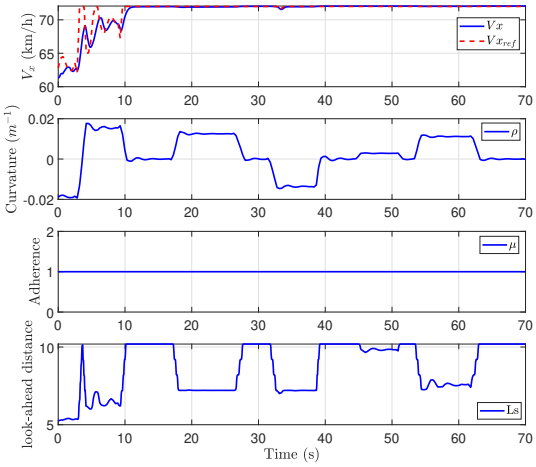

Fig. 9: Ls adapted to V, ρ, μ (Sc1)

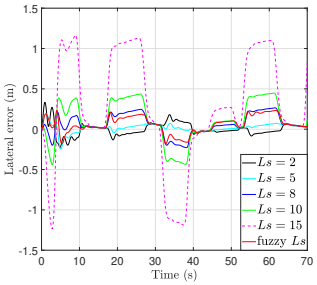

Fig. 10: Lateral Errors (Sc1)

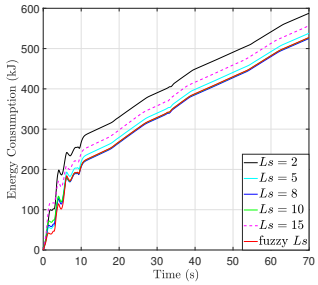

Fig. 11: Consumed Energy(Sc1)

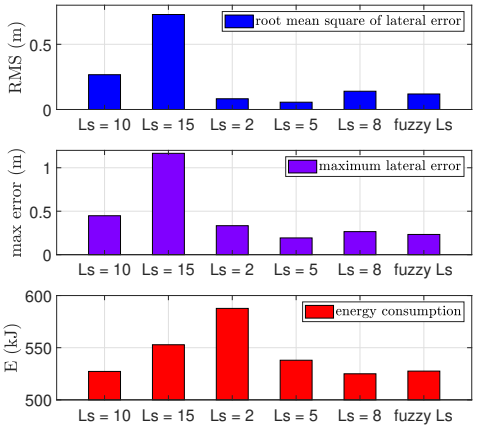

Fig. 12: Cost Variables (Sc1)

While several works proposed to adapt Ls to various parameters, multiple studies have decided to keep Ls constant as in [6], [29]. The developed fuzzy decision approach will be tested and contrasted with other works presented in the literature. In particular, the approach based on tuning Ls as a function of velocity presented in [18] denominated by $f_1(v)$, and the mentioned approaches considering a constant Ls in the path tracking problem. Further, we proposed another method for tuning Ls in terms of velocity (m/s) only, designated by $f_2(v)$ and given by

$$Ls = f_2 = \begin{cases} 3 & \text{if } V \leq 10/3.6 \\ 0.42V + 1.83 & \text{if } 10/3.6 \leq V \leq 70/3.6 \\ 10 & \text{if } V \geq 70/3.6 \end{cases} \quad (12)$$

A case study is performed considering three scenarios. It will be demonstrated that the proposed fuzzy approach exhibits a compromise between energy consumption and tracking performance, and offers supreme stability in case of adherence variation.

A. Scenario 1 (Sc1)

A portion of a realistic trajectory is taken from $SCANeR^{TM}$ studio simulator and presented in Fig. 8. The autonomous vehicle is driven on the track by implementing the lateral controller based on the fuzzy look-ahead distance. The longitudinal control assisted the AV in the path-following by tracking the desired velocity profile Vx_{ref}. Vx_{ref} is reduplicated by a constant to augment the maximum velocity from $60\,km/h$ to $72\,km/h$ in order to alienate the vehicle from its comfortable driving. The initial velocity is set slightly lower than the initial desired one. Road adherence μ is considered a constant equal to 1 representing a normal condition under a dry surface. The resulting fuzzy look-ahead distance is shown in Fig. 9 adapted to the three parameters. Ls ranges from $5\,m$ to $10\,m$ as a variation of V and ρ.

Multiple simulations are performed considering several constant values for Ls and contrasted with our fuzzy approach. It can be observed that there is a nominal value for Ls which reveals the best tracking ($Ls = 5\,m$), where it decays as Ls detaches from this value (Fig. 10). On the other hand, as Ls rises up to a certain limit ($Ls = 10\,m$), the consumed energy by the vehicle decreases (Fig. 11), as the traveled distance becomes shorter. Obviously, there is a trade-off between the path-tracking performance and the energy economy. Figure 12 reveals the Root Mean Square and the maximum lateral errors corresponding to the distinct values of Ls, in addition to the total consumed energy by the AV. RMS is minimal corresponding to low look-ahead distances with a global minimum at $Ls = 5\,m$. The fuzzy Ls ensue $Ls = 2\,m$ by an RMS lower than $Ls = 8\,m$. Similarly for the maximum lateral error except for $Ls = 2\,m$ which exhibited a value greater than the fuzzy Ls. The total energy consumption on the other hand exposes a maximum for $Ls = 2\,m$. The fuzzy Ls exhibited an energy consumption lower than $Ls = 5\,m$, and slightly higher than the $Ls = 8\,m$ case. The case for $Ls = 10\,m$ which revealed an energy consumption similar to the fuzzy Ls is excluded in regards to a high RMS and max error. Therefore,

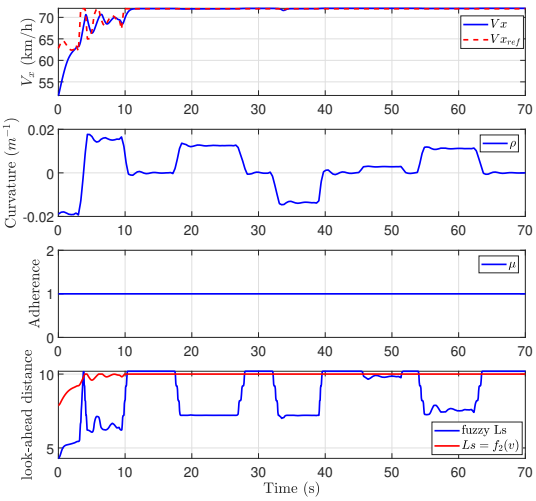

Fig. 13: Ls adapted to V, ρ, μ (Sc2)

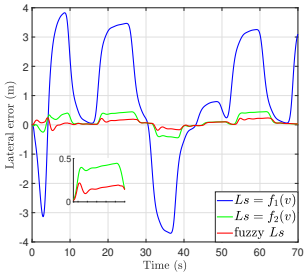

Fig. 14: Lateral Errors (Sc2)

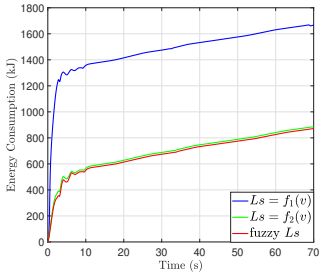

Fig. 15: Consumed Energy(Sc2)

the fuzzy Ls approach manifested a compromise between the path-tracking error and the energy consumption of the AV.

B. Scenario 2 (Sc2)

The second scenario is executed on the same track presented in Fig. 8, with modification of the longitudinal velocity conditions. The scenario is initiated with a velocity lower than the desired and controlled to track the constructed speed profile. Road adherence is set to 1 as before. The fuzzy approach is now compared with the $f_1(v)$ and $f_2(v)$ strategies. The $f_1(v)$ strategy presented in [18] considered tuning Ls to vary from $5m$ to $25m$ as the velocity ranges from $10km/h$ to $50km/h$. The velocity in the case of Sc2 is always above $50km/h$, as it will demonstrate the ineffectiveness of the f_1 strategy. Figure 13 shows the fuzzy Ls and the Ls resulting from $f_2(v)$ as their corresponding parameters vary. $f_1(v)$ reveals an inadmissible behavior in terms of the lateral error Fig. 14 and the energy consumption Fig. 15. Whilst $f_2(v)$ exposes a reasonable lateral error with energy consumption significantly lower than $f_1(v)$. Alternatively, the proposed fuzzy approach elucidated its distinction with the lowest lateral error and energy consumption.

C. Scenario 3 (Sc3)

The last scenario is performed to distinguish the behavior of the AV based on the fuzzy approach in the case of varying road adherence. The road conditions are permanently varying and divided into portions such that: a low adherence ($\mu = 0.45$) on a high curvature, followed by a normal adherence ($\mu = 1$)

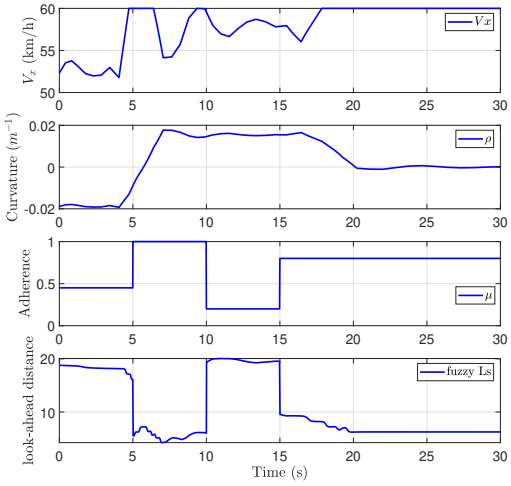

Fig. 16: Ls adapted to V, ρ, μ (Sc3)

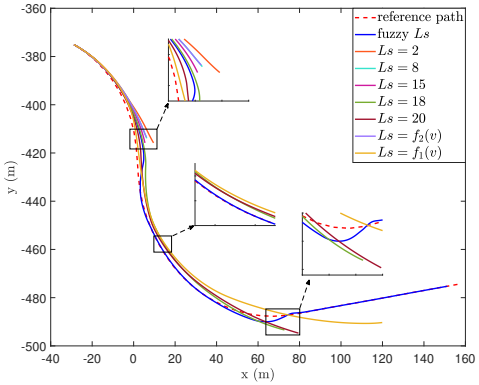

Fig. 17: Trajectories (Sc3)

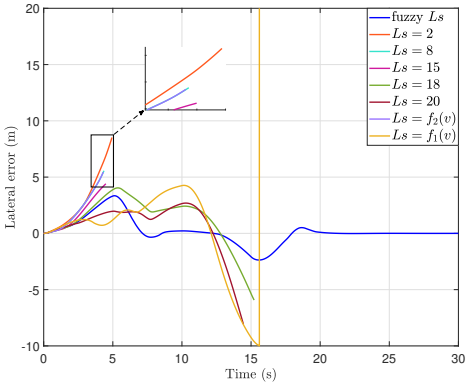

Fig. 18: Lateral Errors (Sc3)

on a combination of low and high curvatures, then extremely low adherence ($\mu = 0.2$) representing a snowy road on high curvature, and finally a moderate adherence ($\mu = 0.8$) on a combination of high and low curvature road. The desired longitudinal velocity, road curvature, road adherence, and the resultant fuzzy look-ahead distance are presented in Figure 16. Several simulations are conducted by assigning distinct constant look-ahead distance values, and assaying the functions

$f_1(v)$ and $f_2(v)$ with the purpose of comparing them with the fuzzy approach. The trajectories of the AV based on the several approaches to tune Ls are presented in Fig. 17, with their associated lateral errors in Fig. 18. It can be observed that besides the fuzzy approach, none of the strategies has succeeded to terminate the test. The road divergence occurs when the AV reaches a level where the lateral error is large and the controller isn't able to further diminish it. Consequently, a complete loss of stability exists and the simulation is ceased. At the first portion of the test (low μ, high ρ), the fuzzy Ls was roughly 18 by dint of Ls_{add}. Hence, $Ls = 2, 8, 15m$ and $Ls = f_2(v)$ were far little from the required value, consequently, the AV diverge from the trajectory. In the second portion, the fuzzy Ls reveals better tracking behavior from the remaining ongoing strategies. In the third portion, the fuzzy Ls was around 20 which is close to the constants $Ls = 18, 20m$, however, $f_2(v)$ was way too large which revealed a cutting-corner phenomenon consequently instability and divergence. At the beginning of the fourth portion, the road condition was significantly altered from $\mu = 0.2$ to 0.8, forcing the fuzzy Ls to attenuate from $20m$ to $10m$ and lesser later when the curvature changed. Hence, the remaining strategies diverge from the road due to their significantly high value.
This test has demonstrated the leading performance of the fuzzy look-ahead distance, and the necessity to consider adapting Ls to the variation of road adherence.

V. Conclusion

In this paper, a fuzzy decision approach is developed to adapt the look-ahead distance of the lateral controller to three parameters, stated as velocity, road curvature, and adherence. It has been demonstrated that for the same controller, under the same test conditions, the performance of the AV significantly alters with the variation of the opted tuning strategy for the look-ahead distance. The proposed fuzzy strategy manifested a compromise between path-tracking performance and energy consumption, and revealed a superior performance in terms of stability and tracking under varying adherence road conditions. Further future works may consider extending the proposed approach to include more parameters or membership functions, and to develop other strategies considering road adherence as a dependent parameter.

ACKNOWLEDGMENT

This work is carried out within the framework of the V3EA project "Electric, Energy Efficient and Autonomous Vehicle" (2021-2025), funded by the Research National Agency (ANR) of the french government.

References

[1] R. Behringer, S. Sundareswaran, B. Gregory, R. Elsley, B. Addison, W. Guthmiller, R. Daily, and D. Bevly, "The darpa grand challenge - development of an autonomous vehicle," in *2004 IEEE Intelligent Vehicles Symposium*, 2004, pp. 226–231.

[2] G. Chen, J. Yao, H. Hu, Z. Gao, L. He, and X. Zheng, "Design and experimental evaluation of an efficient mpc-based lateral motion controller considering path preview for autonomous vehicles," *Control Engineering Practice*, vol. 123, p. 105164, 2022.

[3] H.-S. Tan and J. Huang, "Design of a high-performance automatic steering controller for bus revenue service based on how drivers steer," *IEEE Transactions on Robotics*, vol. 30, no. 5, pp. 1137–1147, 2014.

[4] H. Peng, W. Wang, Q. An, C. Xiang, and L. Li, "Path tracking and direct yaw moment coordinated control based on robust mpc with the finite time horizon for autonomous independent-drive vehicles," *IEEE Transactions on Vehicular Technology*, vol. 69, no. 6, pp. 6053–6066, 2020.

[5] Y. Zou, N. Guo, and X. Zhang, "An integrated path-following and yaw motion control strategy for autonomous distributed drive electric vehicles with differential steering," in *2019 IEEE Intelligent Vehicles Symposium (IV)*, 2019, pp. 1987–1992.

[6] A. Chebly, R. Talj, and A. Charara, "Coupled longitudinal/lateral controllers for autonomous vehicles navigation, with experimental validation," *Control Engineering Practice*, vol. 88, pp. 79–96, 2019.

[7] A. Ollero, A. García-Cerezo, and J. Martínez, "Fuzzy supervisory path tracking of mobile robots1," *IFAC Proceedings Volumes*, vol. 26, no. 1, pp. 277–282, 1993, 1st IFAC International Workshop on Intelligent Autonomous Vehicles, Hampshire, UK, 18-21 April.

[8] S. Qinpeng, W. Zhonghua, L. Meng, L. Bin, C. Jin, and T. Jiaxiang, "Path tracking control of wheeled mobile robot based on improved pure pursuit algorithm," in *2019 Chinese Automation Congress (CAC)*, 2019, pp. 4239–4244.

[9] H. Atoui, V. Milanés, O. Sename, and J. J. Martinez, "Real-time look-ahead distance optimization for smooth and robust steering control of autonomous vehicles," in *2021 29th Mediterranean Conference on Control and Automation (MED)*, 2021, pp. 924–929.

[10] C. M. Kang, S.-H. Lee, and C. C. Chung, "A comparative study of lane keeping system: Dynamic and kinematic models with look-ahead distance," in *2015 IEEE Intelligent Vehicles Symposium (IV)*, 2015, pp. 1038–1043.

[11] R. Wang, Y. Li, J. Fan, T. Wang, and X. Chen, "A novel pure pursuit algorithm for autonomous vehicles based on salp swarm algorithm and velocity controller," *IEEE Access*, vol. 8, pp. 166 525–166 540, 2020.

[12] Q. Cui, R. Ding, C. Wei, and B. Zhou, "Path-tracking and lateral stabilisation for autonomous vehicles by using the steering angle envelope," *Vehicle System Dynamics*, vol. 59, no. 11, pp. 1672–1696, 2021.

[13] F. Xu and T. Shen, "Look-ahead prediction-based real-time optimal energy management for connected hevs," *IEEE Transactions on Vehicular Technology*, vol. 69, no. 3, pp. 2537–2551, 2020.

[14] V. Utkin, "On convergence time and disturbance rejection of super-twisting control," *IEEE Transactions on Automatic Control*, vol. 58, no. 8, pp. 2013–2017, 2013.

[15] R. Rajamani, *Vehicle Dynamics and Control*, 2nd ed. Springer, 2012.

[16] Y. Kuwata, J. Teo, G. Fiore, S. Karaman, E. Frazzoli, and J. P. How, "Real-time motion planning with applications to autonomous urban driving," *IEEE Transactions on Control Systems Technology*, vol. 17, no. 5, pp. 1105–1118, 2009.

[17] S. Campbell, "Steering control of an autonomous ground vehicle with application to the darpa urban challenge," 01 2007.

[18] M. Park, S. Lee, and W. Han, "Development of steering control system for autonomous vehicle using geometry-based path tracking algorithm," *ETRI Journal*, vol. 37, no. 3, pp. 617–625, 2015.

[19] A. Said, R. Talj, C. Francis, and H. Shraim, "Local trajectory planning for autonomous vehicle with static and dynamic obstacles avoidance," in *2021 IEEE International Intelligent Transportation Systems Conference (ITSC)*, 2021, pp. 410–416.

[20] Y. Ahn, S. Shin, M. Kim, and J. Park, "Accurate path tracking by adjusting look-ahead point in pure pursuit method," *International Journal of Automotive Technology*, vol. 22, pp. 119–129, 2021.

[21] Y. Shan, W. Yang, C. Chen, J. Zhou, L. Zheng, and B. Li, "Cf-pursuit: A pursuit method with a clothoid fitting and a fuzzy controller for autonomous vehicles," *International Journal of Advanced Robotic Systems*, vol. 12, no. 9, p. 134, 2015.

[22] K. Hasegawa and E. Konaka, "Three look-ahead distance scheme for lateral control of vision-based vehicles," in *2014 Proceedings of the SICE Annual Conference (SICE)*, 2014, pp. 660–665.

[23] L. Chen, N. Liu, Y. Shan, and L. Chen, "A robust look-ahead distance tuning strategy for the geometric path tracking controllers," in *2018 IEEE Intelligent Vehicles Symposium (IV)*, 2018, pp. 262–267.

[24] R. Rajamani, G. Phanomchoeng, D. Piyabongkarn, and J. Y. Lew, "Algorithms for real-time estimation of individual wheel tire-road friction coefficients," *IEEE/ASME Transactions on Mechatronics*, vol. 17, no. 6, pp. 1183–1195, 2012.

[25] L. Shao, C. Jin, C. Lex, and A. Eichberger, "Robust road friction estimation during vehicle steering," *Vehicle System Dynamics*, vol. 57, no. 4, pp. 493–519, 2019.

[26] S. Kato, S. Tsugawa, K. Tokuda, T. Matsui, and H. Fujii, "Vehicle control algorithms for cooperative driving with automated vehicles and intervehicle communications," *IEEE Transactions on Intelligent Transportation Systems*, vol. 3, no. 3, pp. 155–161, 2002.

[27] E. H. Mamdani, "Applications of fuzzy algorithms for control of a simple dynamic plant," *Proceedings of the IEEE*, 1974.

[28] A. Chokor, R. Talj, A. Charara, H. Shraim, and C. Francis, "Active suspension control to improve passengers comfort and vehicle's stability," in *2016 IEEE 19th International Conference on Intelligent Transportation Systems (ITSC)*, 2016, pp. 296–301.

[29] F. Roselli, M. Corno, S. M. Savaresi, M. Giorelli, D. Azzolini, A. Irilli, and G. Panzani, "H control with look-ahead for lane keeping in autonomous vehicles," in *2017 IEEE Conference on Control Technology and Applications (CCTA)*, 2017, pp. 2220–2225.